

MECHANISM OF PHOTOLUMINESCENCE IN HYDROGENATED AMORPHOUS SILICON DETERMINED BY WIDE-BAND QUADRATURE FREQUENCY-RESOLVED SPECTROSCOPY (QFRS)

T. Aoki*, T. Shimizu, D. Saito, K. Ikeda

Department of Electronics and Computer Engineering, and Joint Research Centre of High-technology, Tokyo Polytechnic University (formerly Tokyo Institute of Polytechnics), Atsugi 243-0297, Japan

A triple-peak photoluminescence (PL) lifetime distribution is found for a-Si:H at low temperature and low photogeneration rates (geminate condition) by quadrature frequency-resolved spectroscopy (QFRS). Using a newly developed wide-band QFRS technique allowing analysis over almost 11 decades in time (2 ns to 160 s), a third lifetime peak, in addition to the well-known double lifetime peaks, is observed in the range 0.1–160 s, and is attributed to distant-pair recombination based on the temperature and generation rate dependence. These results suggest the coexistence of exciton and distant pair recombination even under the geminate condition. At higher temperatures, the distribution becomes a double-peaked one, with peaks due to geminate (non-excitonic) and non-geminate (distant-pair) recombination. The discrepancy between the present results and previous simulations suggests that Coulomb interaction should be included in simulations for a-Si:H, to more precisely account for the experimental observations. The effect of an external magnetic field on the lifetime distribution also supports the involvement of exciton and distant-pair recombination under the geminate condition at low temperature.

(Received December 9, 2004; accepted January 26, 2005)

Keywords: Exciton, Distant-pair, Lifetime, Coulomb interaction, Spin, Magnetic field

1. Introduction

Photoluminescence (PL) is one of most useful properties for studying the recombination mechanisms of photoexcited carriers in amorphous semiconductors. The distribution of PL lifetimes induced by disorder of the amorphous semiconductor can be measured even at low photogeneration rates (G), by means of quadrature frequency-resolved spectroscopy (QFRS) [1]. Boullitrop and Dunstan were the first to identify a double-peak PL lifetime distribution for hydrogenated amorphous silicon (a-Si:H) [2], and the phenomenon was later studied in further detail by Ambros *et al.* [3]. Stachowitz *et al.* suggested the involvement of an exciton in the double-peak lifetime distribution, attributing the short-lived ($\sim \mu\text{sec}$) component to a singlet exciton and the long-lived ($\sim \text{msec}$) component to a triplet exciton [4]. Our group observed a double-peak lifetime distribution for a-Ge:H and chalcogenide glasses (e.g., g-As₂S₃ and a-Se), with the results supporting the exciton model [5-7]. Using a dual-phase double lock-in (DPDL) QFRS technique to measure the PL lifetime in the nanosecond region, our group has also confirmed the absence of a nanosecond peak in the lifetime distribution of a-Si:H [8], and shown that the singlet exciton lifetime ($\sim \mu\text{sec}$), much longer than the radiative dipole-transition time ($\tau_0 \approx 10^{-8}$ s), can be attributed to a discrepancy between the orbital sizes of electrons and holes in the determination of the radiative transition rate [9].

Despite this progress, controversy remains as to whether PL in a-Si:H is due to geminate or non-geminate (distant-pair) recombination. Bort *et al.* [10] discovered a geminate condition at around

*Corresponding author: aoki@ee.t-kougei.ac.jp

$G \approx 10^{19} \text{ cm}^{-3} \text{ s}^{-1}$, below which the peak lifetime (τ) is independent of G such that the steady-state carrier density $n_s = G\tau$ is proportional to G . The intensity of the light-induced electron spin-resonance (LESR), analogous to n_s , is also known to be sub-linearly dependent on G , with an approximate relation $n_s \propto G^{0.2}$ [11]. The distant-pair recombination model predicts this sub-linear G -dependence of the LESR intensity, but cannot explain the G -independent lifetime distribution below the geminate condition [12].

By extending the lifetime detection limits of conventional QFRS, our group investigated the lifetime distribution of a-Si:H over almost 11 decades of time (2 ns to 160 s) and discovered a third peak at 0.1–100 s. This third lifetime peak decreased continuously with increasing G , even far below the geminate condition, demonstrating a sublinear G -dependence of n_s in agreement with the LESR results [13].

The lifetime distributions are further investigated in this study and compared with the simulations by Levin *et al.* [14]. The distribution is revealed to be triple-peaked at low temperatures and double-peaked at high temperatures. The effect of a magnetic field on the PL lifetime distribution of a-Si:H at low temperature is also examined. The results support the involvement of exciton and distant-pair recombination in PL generation in a-Si:H at low temperatures, under the geminate condition.

2. Experimental details

A film of a-Si:H with a defect density of $2 \times 10^{16} \text{ cm}^{-3}$ was deposited to a thickness of $1.1 \mu\text{m}$ on a roughened Al substrate. Photoluminescence was excited by irradiation with a 2.33 or 1.81 eV low-noise laser, and the integrated or dispersed PL was detected by an infrared (IR) photomultiplier tube (PMT; R5509-42, Hamamatsu) at photon energies of 0.89 eV or greater. The PL lifetime distributions were measured by QFRS over almost 11 decades in time, from 2 ns to 160 s. The shorter (up to $\sim \mu\text{sec}$) lifetimes were measured by the DPDL QFRS technique, as illustrated in Fig. 1 [8]. An electro-optic modulator (EOM; 50, Conoptics) was employed to modulate the laser beam at up to 80 MHz, instead of the usual acousto-optic modulator (AOM). As electromagnetic interference between the rf digital lock-in amplifier (SR844, Stanford Research System) and the EOM driver became serious at rf frequencies (ω) above 10 MHz, the laser beam was chopped at 8 Hz (ω_m) and the PL signal was discriminated from the interference by lock-in detection at ω_m . The doubly modulated PL signal is expressed as

$$S(t) = R(\omega) \sin(\omega t - \theta(\omega)) \cdot \sin(\omega_m t) \quad (1)$$

where $R(\omega)$ and $\theta(\omega)$ are the PL amplitude and phase at ω , respectively. The lifetime distribution is principally given by the quadrature part ($R(\omega) \sin\theta(\omega)$) in QFRS. However, as $R(\omega)$ and $\theta(\omega)$ include components of the instrumental response due to the EOM, PMT, and optical and electrical lengths, the quadrature signal was calibrated as mentioned later.

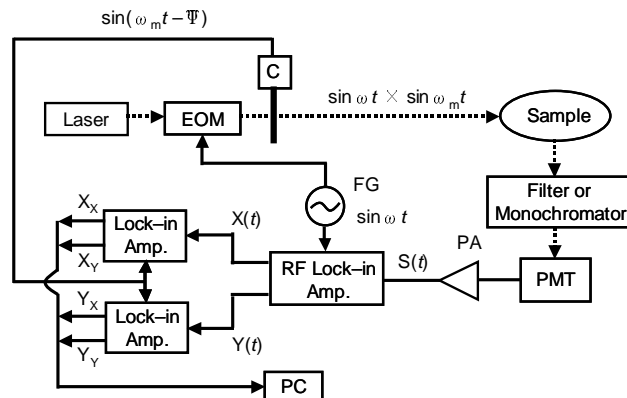


Fig. 1. Schematic diagram of the DPDL QFRS technique (C, optical chopper; FG, function generator; PA, preamplifier; PMT, photomultiplier tube; PC, personal computer).

The rf lock-in amplifier was locked at ω , and had a low-pass filter (LPF) time constant $\gg \omega^{-1}$ and $\ll \omega_m^{-1}$. The X - and Y -channel outputs were sinusoidal, with frequency ω_m , as given by

$$\left. \begin{aligned} X(t) &= \frac{1}{2} R(\omega) \cos \theta(\omega) \sin(\omega_m t) \\ Y(t) &= \frac{1}{2} R(\omega) \sin \theta(\omega) \sin(\omega_m t) \end{aligned} \right\} \quad (2)$$

These signals were again synchronously detected at ω_m using two digital lock-in amplifiers (SR830) with LPF time constants of much greater than ω_m^{-1} . A phase shift ψ was inserted between the chopped light and the synchronous signal of the chopper driver (Fig. 1). Eliminating ψ from the X - and Y -channel outputs of the two lock-in amplifiers (X_X , X_Y , Y_X and Y_Y), $R(\omega)$ and $\theta(\omega)$ could be obtained as follows.

$$\left. \begin{aligned} R(\omega) &= 4\sqrt{X_X^2 + X_Y^2 + Y_X^2 + Y_Y^2} \\ \theta(\omega) &= \frac{1}{2} \left(\tan^{-1} \frac{Y_X + X_Y}{X_X - Y_Y} + \tan^{-1} \frac{Y_X - X_Y}{X_X + Y_Y} \right) \end{aligned} \right\} \quad (3)$$

Measuring the instrumental $R'(\omega)$ and $\theta'(\omega)$ of the modulated laser light reflected at an Al plate instead of the sample, the intrinsic QFRS signal of PL was obtained as

$$R(\omega) \sin(\theta(\omega) - \theta'(\omega)) / R'(\omega) \quad (4)$$

The DPDL QFRS technique has been shown to resolve PL lifetimes \sim nsec, through observations of the fluorescence of Rhodamine 6G, which has a PL lifetime of 4 ns [15].

Longer lifetimes up to 160 s were measured using an AOM coupled with the SR830 digital lock-in amplifier in internal mode, with synchronous filtering to avoid phase noise. Fibre optics was employed to avoid magnetic field disturbances at the PMT. PL lifetime distributions were also obtained under external magnetic fields of up to 0.9 T for an a-Si:H film deposited on a Corning 7059 glass substrate, by illuminating the glass side of the sample and detecting the PL from the opposite side.

3. Results and discussion

The results of the present ultra wide-band QFRS measurements, extending far below the geminate recombination condition ($G < 10^{19} \text{ cm}^{-3} \text{ s}^{-1}$), are shown in Fig. 2, for photoexcitation energies (E_X) of 2.33 eV (above-bandgap excitation) and 1.81 eV (bandgap excitation). Darkened areas in the figure indicate lifetime ranges extended by the present work. The PL lifetime distributions are triple-peaked at $T \leq 20$ K, but become double-peaked (τ_g and τ_{ng}) at approximately 100 K, regardless of E_X . This can be explained by the coexistence of exciton (i.e., geminate pair) and non-geminate (i.e., distant-pair) recombination at low temperatures, and geminate (non-excitonic) and non-geminate recombination at higher temperatures [13]. The exciton model attributes the short-lifetime peak τ_S to a singlet exciton and the long-lifetime peak τ_T to a triplet exciton at low temperatures [4-7]. It has been reported for a-Si:H that self-trapped holes become unstable with increasing temperature, accompanied by a disappearance of the triplet self-trapped exciton at around 85 K [16]. This corresponds to the disappearance of the τ_T peak at around 80 K in Fig. 2. The smaller binding energy of the singlet exciton, related to the exchange energy, is responsible for the disappearance of the τ_S peak at $T \geq 30$ K. At approximately 40 K, τ_g develops as a shoulder between τ_S and τ_T , growing to a new peak at higher temperature [13].

The third peak τ_{ng} , occurring at 1 s at 3.7 K, may have been overlooked in the past, due to the limitations of QFRS at very low frequencies. This third peak is attributable to non-geminate or distant-pair recombination [13]. It is selectively enhanced with increasing temperature, leading to the establishment of a double-peak distribution with maxima at τ_g and τ_{ng} at around 100 K under both excitation conditions.

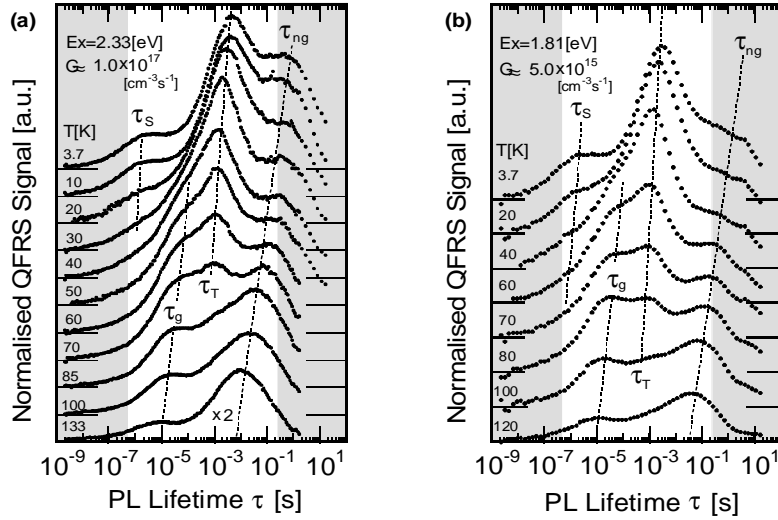


Fig. 2. QFRS spectra of a-Si:H photoexcited at (a) $E_X = 2.33$ eV with $G \approx 1.0 \times 10^{17} \text{ cm}^{-3} \text{ s}^{-1}$ and (b) $E_X = 1.81$ eV with $G \approx 5.0 \times 10^{15} \text{ cm}^{-3} \text{ s}^{-1}$. Darkened regions are lifetime ranges extended by the present work.

Fig. 3 shows plots of the peak lifetime τ_{ng} against G at 3.7 K, for comparison with previously reported values of τ_s and τ_T [9]. The continuous reduction of τ_{ng} with increasing G suggests the occurrence of non-geminate recombination, even far below the geminate condition ($G < 10^{19} \text{ cm}^{-3} \text{ s}^{-1}$). The τ_{ng} fit to the curve was calculated from the balance equation determining the steady-state carrier density n_s [17,18] assuming a radiative dipole transition time τ_0 of 10^{-8} s, an effective electron localization radius a of 10 \AA , and ignoring the radii of holes. As G increases from 10^{13} to $10^{22} \text{ cm}^{-3} \text{ s}^{-1}$, at which the a-Si:H film starts photodegrading, τ_{ng} continuously decreases even below the geminate condition where τ_s and τ_T remain constant.

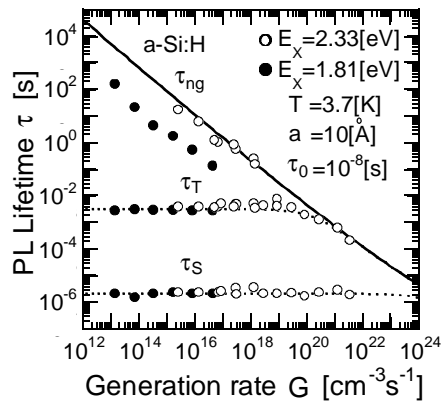


Fig. 3. Peak lifetimes τ_s , τ_T and τ_{ng} as functions of G at 3.7 K with E_X of (○) 2.33 and (●) 1.81 eV.

Similar plots for the double-peak lifetime distribution at 100 K are shown in Fig. 4. As G increases, the lifetime τ_{ng} continuously decreases and finally merges with τ_g , which remains constant against G . The curve of τ_{ng} as a function of G , obtained from the balance equation assuming $a = 42 \text{ \AA}$, fits the plots well, although the validity of the equation at high temperature is unclear, as both down-hops and up-hops of photoexcited carriers will occur in the tails and non-radiative recombination can no longer be ignored. The τ_g peak is situated between τ_s and τ_T (Fig. 2) and remains constant with increasing G up to $\approx 10^{20} \text{ cm}^{-3} \text{ s}^{-1}$ (Fig. 4). Therefore, the peak at τ_g is thought

to originate from geminate recombination at high temperature, where thermal disturbance prevents an electron-hole pair from forming an exciton, even though the pair is geminate. The value of τ_g between 10^{-5} and 10^{-4} s is in agreement with that given by $\tau_0(v_0\tau_0)^{0.8} \approx 1.6 \times 10^{-5}$ s based on electron-hole separation that maximises the geminate recombination function assuming a phonon frequency v_0 of 10^{12} s $^{-1}$ order, although the temperature is not low ($T \approx 100$ K) [17].

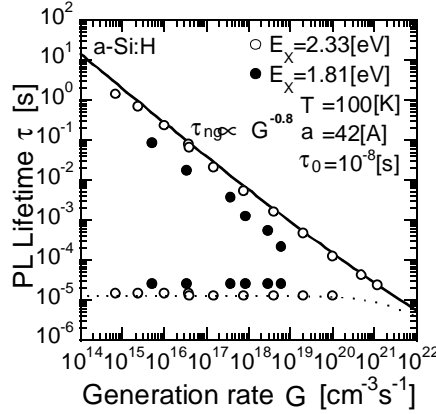


Fig. 4. Peak lifetimes τ_g and τ_{ng} as functions of G at 100 K with $E_X = (\circ)$ 2.33 eV and (\bullet) 1.81 eV.

The occurrence of geminate recombination at temperatures as high as 100 K, and the stronger non-geminate component τ_{ng} at $E_X = 2.33$ eV compared to $E_X = 1.81$ eV, can be explained using a classical Onsager model. It is assumed that an electron is excited to an energy $E_X - E_g$ above the mobility gap E_g and a hole is fixed at the location where the electron-hole pair was generated. Emitting phonons of energy $h\nu_0$, the electron will diffuse a distance r_d given by [19]

$$r_d = \left[\frac{D \left(E_X - E_g + \frac{e^2}{4\pi\epsilon r_d} \right)}{h\nu_0^2} \right]^{1/2} \quad (5)$$

before it is thermalised. Here, D is the electron diffusion constant given by $\mu kT/e$ in terms of the electron mobility μ , and ϵ is the dielectric constant of a-Si:H. After thermalisation, the electron-hole Coulomb energy becomes $e^2/4\pi\epsilon r_d$. If this is lower than the thermal energy kT , the electron will escape from the hole and recombine with another one (non-geminate or distant-pair recombination). If $e^2/4\pi\epsilon r_d > kT$, the electron cannot escape from the hole created by the photon, resulting in geminate recombination. The electron-escape probability can be expressed as

$$p \approx \exp\left(-\frac{e^2}{4\pi\epsilon r_d kT}\right) \quad (6)$$

The relative quantum efficiency (QE) η is obtained by dividing the area of the τ_{ng} component by the total area of the τ_s , τ_T , and τ_{ng} components at low temperature, and by the total area of the τ_g and τ_{ng} components at high temperature, as in Fig. 2. The values obtained are plotted as a function of T in Fig. 5. The electron-escape probability p is estimated using $\mu = 10$ cm 2 /V s and E_g as obtained from Tauc plots for various temperatures. The quantum efficiency of distant-pair recombination and the electron-escape probability increase with T , and both η and p are larger at higher E_X . Thus, although nonradiative recombination at high temperature is ignored, the T and E_X dependences of the τ_{ng} component can be explained by the distant-pair model. The discrepancy between p and the measured η at low T is due largely to a disregard for hopping diffusion in the band tails in Eq. (5).

Fig. 5 also shows that the QE of geminate or excitonic recombination is about 60%, compared with the value of 20% predicted by simulation for low temperature and a photogeneration

rate of $G \approx 10^{17} \text{ cm}^{-3} \text{ s}^{-1}$ [14], and that geminate recombination takes place even at temperatures greater than 100 K (Fig. 2). The discrepancy between the present experimental results and the theoretical calculations is probably due to the omission of Coulomb interaction between electrons and holes in the simulations [14]. As Coulomb attraction is essential for the formation of the exciton, spin effects as well as Coulomb interaction should be included in order to obtain a more complete theoretical description of the PL lifetime distributions for a-Si:H.

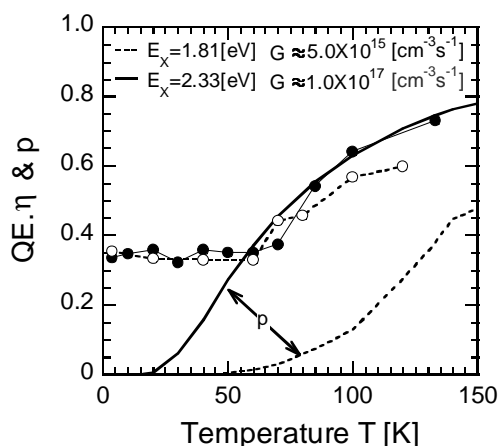


Fig. 5. Plots of η and p as functions of T at E_X of (●, solid) 2.33 eV with $G \approx 1.0 \times 10^{17} \text{ cm}^{-3} \text{ s}^{-1}$ and E_X of (○, dotted) 1.81 eV with $G \approx 5.0 \times 10^{15} \text{ cm}^{-3} \text{ s}^{-1}$.

The steady-state carrier density $n_s = \eta_{\text{ng}} G \tau_{\text{ng}}$ calculated using η_{ng} is proportional to $G^{0.17}$ and agrees with the LESR results reported previously [13]. The variation of n_s with temperature also agrees quite well with the temperature dependence of the LESR data [13]. These results support the notion that the τ_{ng} component originates from distant-pair recombination.

Fig. 6 shows the PL spectra of the QFRS signals obtained for a-Si:H at 3.7 K, at frequencies of 72.3 kHz, 49.7 Hz and 0.280 Hz, corresponding to $\tau_S \approx 2.2 \mu\text{s}$, $\tau_T \approx 3.2 \text{ ms}$ and $\tau_{\text{ng}} \approx 0.57 \text{ s}$, respectively. The PL peak associated with the short-lived component τ_S occurs at a photon energy about 40 meV higher than that for the long-lived component τ_T . This difference is attributable to the exchange energy as reported previously [9]. The PL spectrum of τ_{ng} peaks at a slightly lower photon energy than that of τ_T . Therefore the electron-hole state is deep in the tail before recombining with a lifetime τ_{ng} . On the other hand, LESR only measures some fraction of the light-induced carriers in the tails (i.e., deeply trapped carriers [20]). Thus the PL spectrum of the τ_{ng} component obtained here can be correlated with the LESR signal, revealing that the τ_{ng} component appears to obey the distant-pair recombination model.

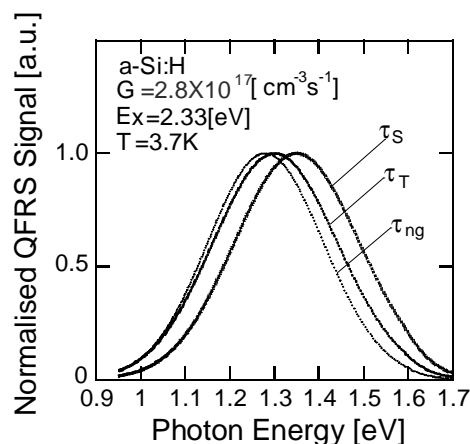


Fig. 6. QFRS PL spectra for the τ_S (72.3 kHz), τ_T (49.7 Hz) and τ_{ng} (0.280 Hz) lifetime peaks with $G \approx 2.8 \times 10^{17} \text{ cm}^{-3} \text{ s}^{-1}$. All the peaks of spectra are normalised to unity.

The dependence of the PL lifetime distribution of a-Si:H at 3.7 K on the intensity of an external magnetic field is shown in Fig. 7. Application of a 0.9 T magnetic field weakens the QFRS signal of the τ_{ng} component, and enhances that of the τ_T component, but has little influence on the τ_S component (Fig. 7(a)). This tendency is clarified in Fig. 7(b), which shows plots of the QFRS signals of the three components measured at 2 μ s, 3 ms and 80 ms as functions of the magnetic field intensity.

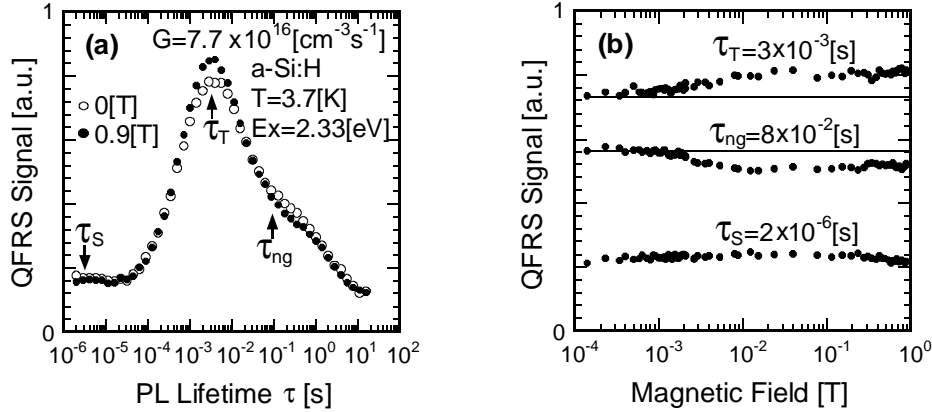


Fig. 7. (a) Lifetime distributions at 3.7 K and $G = 7.7 \times 10^{16} \text{ cm}^{-3} \text{ s}^{-1}$, with (\circ) and without (\bullet) the application of a 0.9 T magnetic field. (b) QFRS signals of the τ_S , τ_T and τ_{ng} components as functions of the magnetic field intensity.

Based on transient PL, Robins and Kastner observed an enhancement of the triplet exciton recombination and a decrease in distant-pair recombination for both amorphous and crystalline As_2Se_3 under a magnetic field, and suggested an explanation for the results [21]. They observed no singlet exciton state in this material, which our group has also confirmed by DPDL QFRS [6]. In our analyses, the application of a 0.9 T external magnetic field to a- As_2Se_3 was also shown to strengthen the τ_T component and weaken the τ_{ng} component.

Following [21], the results shown in Fig. 7 are explained in terms of an excitonic model for the τ_S and τ_T components. As a singlet exciton has a total spin of zero ($S = 0$), the τ_S component assigned to the singlet exciton is unaffected by the application of a magnetic field. The three-fold degeneracy of the triplet exciton ($S = 1$) is removed by the anisotropic spin-spin interaction and spin-orbit interaction, causing a zero-field splitting in the absence of an external magnetic field. Each of the three eigenstates couples differently with the excited singlet states, allowing relaxation to the singlet ground state with lifetimes specific to each state. Furthermore, the Zeeman interaction with the magnetic field mixes the zero-field eigenstates and further separates their energies, thereby changing the lifetime of the triplet exciton. Thus, the enhancement of the τ_T component under a magnetic field is due to the involvement of triplet exciton recombination in a-Si:H, similar to the case of a- As_2Se_3 .

In the absence of an external magnetic field, the spin directions of the distant pair are completely random. That is, the total spin S is not a good quantum number because of the lack of correlation in the pair. When a magnetic field is applied, the spins of the carriers will have a finite polarization [22]. Then, as the spin-aligned state which is energetically favoured under a magnetic field is spin-forbidden to recombine, the recombination rate will decrease. In contrast, the formation of a pair in an anti-parallel spin-allowed state is slightly inhibited by the magnetic field. Overall, the distant-pair recombination rate will be reduced by the application of an external magnetic field, resulting in the weakening of the τ_{ng} component seen in Fig. 7.

4. Conclusions

A triple-peak PL lifetime distribution for a-Si:H, in addition to the well-known double-peak distribution, was observed under the geminate condition at low temperatures, by ultra wide-band

QFRS. The triple-peak lifetime distribution indicates the involvement of a distant pair in recombination events, in addition to singlet and triplet excitons. The lifetime of the distant-pair recombination as a function of the generation rate can be accurately predicted by the balance equation over the full range of G , even at higher temperatures. The temperature dependence of the triple-peak lifetime distribution was found to be explicable by a model involving three different types of recombination. At higher temperatures (ca. 100 K), the distribution becomes the double-peak distribution, with geminate and non-geminate recombination peaks. Although excitons are no longer formed above 100 K, the geminate pair persists. These results indicated that Coulomb interaction, essential for the formation of both excitons and geminate pairs, should be included in simulations of the PL lifetime distributions for a-Si:H. The application of a 0.9 T magnetic field was found to weaken distant-pair recombination and enhance triplet exciton recombination, yet was found to have little influence on singlet exciton recombination. These observations were well explained by spin effects on electron-hole pairs.

Acknowledgements

This work was carried out in cooperation with Gifu University (Prof. K. Shimakawa). The authors thank the Promotion and Mutual Aid Corporation for Private Schools of Japan for financial assistance from the Scientific Research Promotion Fund.

References

- [1] S. P. Depinna, D. J. Dunstan, *Philos. Mag.* **B50**, 579 (1984).
- [2] F. Boulitrop, D. J. Dunstan, *J. Non-Cryst. Solids* **77 & 78**, 663 (1985).
- [3] S. Ambros, R. Carius, H. Wagner, *J. Non-Cryst. Solids* **137 & 136**, 555 (1991).
- [4] R. Stachowitz, M. Schubert, W. Fuhs, *J. Non-Cryst. Solids* **227-230**, 190 (1998).
- [5] S. Ishii, M. Kurihara, T. Aoki, K. Shimakawa, J. Singh, *J. Non-Cryst. Solids* **266-269**, 721 (2000).
- [6] T. Aoki, S. Komodoori, S. Kobayashi, T. Shimizu, A. Ganjoo, K. Shimakawa, *J. Non-Cryst. Solids* **326 & 327**, 273 (2003).
- [7] J. Singh, T. Aoki, K. Shimakawa, *Philos. Mag.* **B82**, 855 (2002).
- [8] T. Aoki, S. Komodoori, S. Kobayashi, C. Fujihashi, A. Ganjoo, K. Shimakawa, *J. Non-Cryst. Solids*, **297-302**, 642 (2002).
- [9] T. Aoki, *J. Mater. Sci. –Materials in Electronics* **14**, 697 (2003).
- [10] M. Bort, W. Fuhs, S. Liedtke, R. Stachowitz, R. Carius, *Philos. Mag. Lett.* **64**, 227 (1991).
- [11] F. Boulitrop, D. J. Dunstan, *Solid State Commun.* **44**, 841 (1982).
- [12] D. J. Dunstan, *Philos. Mag.* **B52**, 111 (1985).
- [13] T. Aoki, T. Shimizu, S. Komodoori, S. Kobayashi, K. Shimakawa, *J. Non-Cryst. Solids* **338-340**, 456 (2004).
- [14] E. I. Levin, S. Marianer, B. I. Shklovskii, *Phys. Rev.* **B45**, 5906 (1992).
- [15] T. Aoki, S. Komodoori, S. Kobayashi, T. Shimizu, A. Ganjoo, K. Shimakawa, *Nonlinear Optics* **29(4-6)**, 273 (2003).
- [16] K. Morigaki, M. Yamaguchi, I. Hirabayashi, *J. Non-Cryst. Solids*, **164-166**, 571 (1993).
- [17] B. I. Shklovskii, H. Fritzsche, S.D. Baranovskii, *Phys. Rev. Lett.* **62**, 2989 (1989).
- [18] T. M. Searle, *Philos. Mag. Lett.*, **61**, 251 (1990).
- [19] N. F. Mott, E.A. Davis, *Electronic Processes in Non-Crystalline Materials*, Clarendon Press, Oxford U.K. (1979).
- [20] B. Yan, P. C. Taylor, *Mat. Res. Soc. Symp. Proc.* **507**, 805 (1998).
- [21] L. H. Robins, M. A. Kastner, *Phys. Rev.* **B35**, 2867 (1987).
- [22] I. Solomon, *Topics in Applied Physics, Amorphous Semiconductors*, Ed. M.H. Brodsky, Springer, Berlin Heidelberg New York, **36**, 189 (1979).